2020 IEEE/RSJ International Conference on Intelligent Robots and Systems (IROS)
October 25-29, 2020, Las Vegas, NV, USA (Virtual)

A Two-stage Automatic Latching System for The USVs Charging in Disturbed Berth

Kaiwen Xue[2,†], Chongfeng Liu[2,†], Hengli Liu[3], Ruoyu Xu[2]
Zhenglong Sun[1,2], Tin Lun Lam[1,2], Huihuan Qian[1,2,‡]

***Abstract*— Automatic latching for charging in a disturbed environment for Unmanned Surface Vehicle (USVs) is always a challenging problem. In this paper, we propose a two-stage automatic latching system for USVs charging in berth. In Stage I, a vision-guided algorithm is developed to calculate an optimal latching position for charging. In Stage II, a novel latching mechanism is designed to compensate the movement misalignments from the water disturbance. A set of experiments have been conducted in real-world environments. The results show the latching success rate has been improved from 40% to 73.3% in the best cases with our proposed system. Furthermore, the vision-guided algorithm provides a methodology to optimize the design radius of the latching mechanism with respect to different disturbance levels accordingly. Outdoor experiments have validated the efficiency of our proposed automatic latching system. The proposed system improves the autonomy intelligence of the USVs and provides great benefits for practical applications.**

I. INTRODUCTION

Unmanned Surface Vehicles (USVs) have a range of applications in ports, such as rescue missions, monitoring waterways and underwater situations, logistic support, and so on [1]. There is a great need to deploy USVs in ports or coastal areas [2]. The full-autonomy of USVs will accelerate their deployment and speed up the future development progress of USVs. But this requires USVs to complete the specified tasks like patrolling, berthing as well as energy replenishment with no human intervention.

As for energy replenishments, the main technical hurdles associated with automatic charging for USVs include the accurate positioning of the USV latching mechanism, and the reliable latching of the USV [3]. After solving the two hurdle tasks, the following charging procedure can be further implemented. Lots of automatic charging techniques have been developed for Unmanned Aerial Vehicles (UAVs), Automatic Guided Vehicles (AGVs) and Autonomous Underwater Vehicles (AUVs). Compared with those, solutions for USVs are less studied to date. Since charging on the water surface will be severely disturbed from the waves, currents and winds consistently, this makes the automatic latching and charging procedures differ from other unmanned systems. In terms of USV, automatic latching for charging still needs more investigation.

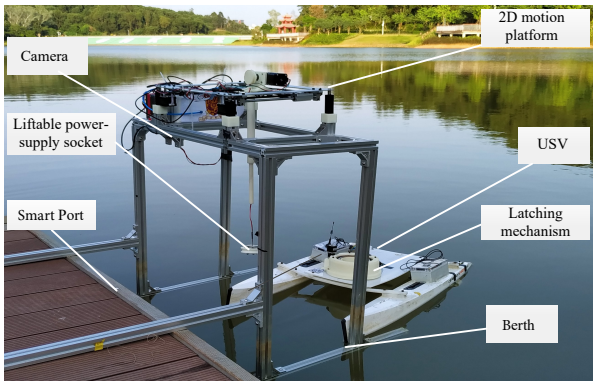

Fig. 1. A USV docks at the berth and performs the automatic latching and charging operation for further tasks in a berth.

To be more specific, when a USV returns to ports and docks at the berth for charging, it is worth considering how to connect the power plug with the power socket automatically and reliably in such a multi-disturbance environment. On the other hand, the automatic recharging for USVs will increase the intelligence capability of the ports and facilitate USVs to achieve full autonomy in berth [4]. With these motivations, in this paper we propose a two-stage vision-guided automatic latching system for USVs charging in ports.

The challenges of charging for autonomous systems in disturbance mainly consist of positioning and latching. These two problems have attracted much interest of related research in aerial [5], ground [6] and underwater [7] areas. Among the techniques of positioning in short range, especially for positioning with accuracy of centimeter level, vision sensors are dominant among other sensors [8][15]. As for the latching method, it can be divided into different types of mechanism, such as the pole and latch type, permanent magnet type, pyramid type and funnel type [6][14]. In [9], a single camera is used to help the USV to cooperate with the underwater vehicle to finish its docking manoeuvre. Real-time pose tracking is developed by using stereo vision and 3D markers [18] [19]. In [7], an AUV docks to the seafloor station autonomously for battery charging based on four LED markers. In another study [17], an Extended Kalman Filter (EKF) algorithm is used in the positioning process during the latching procedure. In underwater environments, most researches tend to solve the problem of positioning

This paper is partially supported by Project U1613226 and U1813217 supported by NSFC, China, Project 2019-INT009 from the Shenzhen Institute of Artificial Intelligence and Robotics for Society, the Shenzhen Science and Technology Innovation Commission, fundamental research grant KQJSCX20180330165912672 and PF.01.000143 from The Chinese University of Hong Kong, Shenzhen.

†These two authors contribute equally to this paper.
[1]Shenzhen Institute of Artificial Intelligence and Robotics for Society, Shenzhen, China.
[2]The Chinese University of Hong Kong, Shenzhen.
[3]Peng Cheng Laboratory, Shenzhen, China.
‡Corresponding author is Huihuan Qian, email: hhqian@cuhk.edu.cn

by obtaining higher resolution images with stereo vision algorithms. Compared with positioning, less work has been done for the design of the latching mechanism. As for surface vehicle latching operation, Scott et al. [10] proposes a latching system with vision and a robotic arm for refueling. A magnet installed on the end effector of a robotic arm is acting as a latching device. However, this system needs nylon ropes to stabilize the USV in advance. Besides, after refueling, the magnet can be considered be removed automatically in the future instead of removing manually as depicted in this paper. For robotic boat in [11], a novel latching mechanism based on a spherical joint (ball and socket) is designed to enable the USVs to unite dynamically and compensate the misalignments in disturbed water environments. This work shows a satisfying performance that it can be further developed for the purpose of charging. However, the size of the latching mechanism with respect to the boat size can be further discussed to optimize the latching mechanism design.

In terms of latching and charging system of USV in berth, the latching error comes from two main sources. First, the environment dynamics model of both waves and currents is rapidly changing and hard to predict accurately in water. Another difficulty comes from the constrained movement in a berth. The movement will be subject to the collision force when the USV is colliding with the berth during its movement.

This paper presents a vision-guided automatic latching system for charging of USVs in ports, as shown in Fig.1. Different from others which mainly focus on the pose tracking, our proposed system combines the novel algorithm and the innovation on mechanism and can be easy to implement. The main features in our systems are: (1) a vision-guided algorithm solves the positioning for latching based on position sampling and optimization of the latching mechanism centers. (2) a novel latching mechanism compensates certain misalignments from disturbances. (3) the proposed algorithm can further optimize the design of the latching mechanism. Our proposed system has been tested in outdoor environment and achieves satisfying results.

The rest of this paper is organized as follows. Section II gives an overview of the proposed system. The vision-guided algorithm will be introduced in Section III. Section IV will illustrate the latching mechanism design and its optimization. The experiment setup and results are presented in Section V. Conclusions and future works are summarized in Section VI.

II. Latching System Overview

The latching system enables automatic charging for USVs in a berth. The proposed latching system mainly consists of vision-guided positioning and automatic latching for USVs charging, which is defined as two stages in our system. This section will present an overview introduction about the proposed two-stage solution in the system. Then the design of the vision-guided positioning algorithm will be further illustrated in Section III. The description of the latching mechanism design and optimization will be introduced in Section IV.

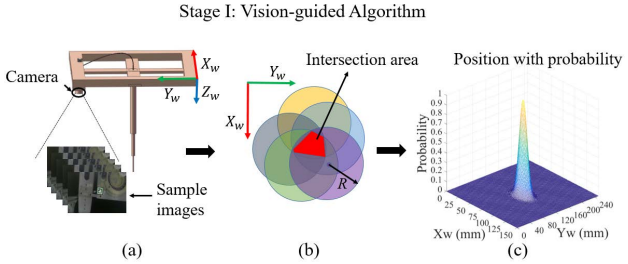

Fig. 2. Latching system overview: Stage I vision-guided algorithm (a) Sample k images of the USV by using AprilTag. (b) Find the intersection area with latching mechanism design radius R. (c) Apply the proposed vision-guided algorithm to find the optimal position with probability.

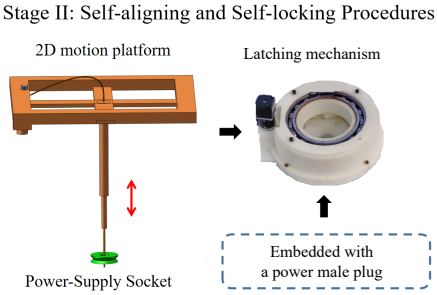

Fig. 3. Latching system overview. After getting the optimal position in Stage I, the 2D motion platform (mounted on the berth) will guide the power-supply socket to the latching mechanism. Subsequently, the mechanism performs self-aligning and self-locking procedures.

Fig.2 and Fig.3 show the overall two-stage latching system design. The proposed system hardware mainly includes a camera, an Apriltag marker [12], a 2D motion platform and a latching mechanism. The Apriltag marker and latching mechanism are attached to the surface of the USV, so that the position information of the latching mechanism can be obtained.

In stage I, as shown in Fig.2, the camera takes k sample images first and then detects the Apriltag marker to position the center of the latching mechanism. Then these centers will be used to find the intersection area, where R is the design radius of the latching mechanism, which will be illustrated in Section III. Then the intersection area will be further used to calculate the optimal latching position with probability. In Fig.3, a power plug connected with battery is mounted at the center of the latching mechanism. Thus, the calculated optimal position is the goal position where the power-supply socket to enter. In stage II shown in Fig.3, the 2D motion platform will first lower down the power-supply socket to maintain a reasonable distance from the USV and make sure the instant and timely operation. By this pre-operation, the following charging operation will be guaranteed to be timely enough in our experiments even without using a time-demanding control methods like visual servo methods. Subsequently, the latching mechanism will align the power-supply socket to the center and then lock it. A pair of round-head power interfaces is embedded respectively in the power-supply socket and the plug, as the dotted frame shows in Fig.3. Thus, after latching, the power-supply socket have mated with the male plug in the latching mechanism on the

USV and the charging procedure can start.

III. Vision-Guided Algorithm Design

The modeling of waves are highly nonlinear and accurate modeling are even not fully understood by the research community by far [20], considering the weather, wind, tide and so on. Furthermore, the measurement of the waves comes in hours, days and even weeks. The lack of real-time wave data makes it extremely difficult for the control and positioning of the USV. All these realities demand an alternative way to find the accurate position of the latching system for charging of USVs. In berth, the USVs movement is usually subject to the disturbances from the water environments, even collision bouncing forces against the berth, making it a great challenge to predict and track the USV precisely. Luckily, the movement of the USV is constrained within the berth, and these berth constraints make the movement of the USV tractable to some extend. Therefore, a different method is used to position the boat for the charging in this section.

In this paper, we focus on the USV positioning within the berth, in which the USVs movement is relatively mild compared to that in the open water. The latching mechanism is designed in small size and aimed to latch the charging mechanism to the USV. A sampling-based and optimization vision-guided algorithm is proposed to tackle the challenging positioning problem without formulating the dynamics model of the USV and water disturbances in the complex water environments.

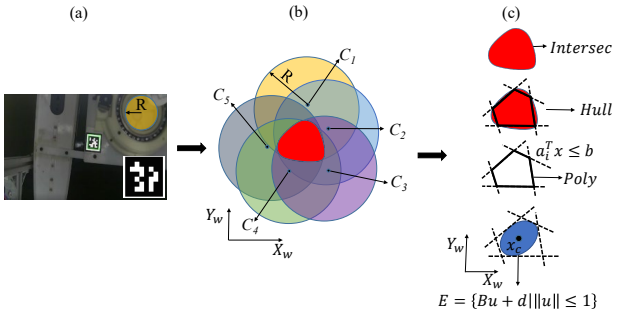

Fig. 4. (a) For example, AprilTag samples $k = 5$ center positions; (b) intersection area is calculated by circles with the specified latching mechanism radius R; (c) Polygon represents feasible intersection area, and the optimization ellipsoid E is used to find the optimal position x_c.

As shown in Fig.4, the USV movement is mild within the berth and the latching mechanism radius R is large with respect to the power-supply socket size. There will exist an intersection area in most cases. The intersection area is the area which will guarantee high success latching operation if the area is large enough to let through the power supply socket. By taking advantage of it, we propose the optimal latching position algorithm within the intersection area using simple and effective methods instead of time-demanding visual servo methods.

A. Data Sampling Procedure

Data sampling is used to sample the movements of the USVs in berth for a period of time, representing the movement of the USV. As shown in Fig.4 (a) and (b), based on the k sample movements of the center C_k of the latching mechanism onboard as well as the latching mechanism radius R, we get the feasible intersection. Based on the intersection, we want to find the optimal position for the power-supply socket to connect the latching mechanism on the USV.

B. Problem Formulation and Optimization

As shown in Fig.4(c), the vision-guided positioning algorithm utilizes the sample positions and uses a convex hull $Hull$ to approximate the intersection area $Intersec$. The convex hull can be further approximated as a combination of a set of halfspaces l_i:

$$l_i : a_i^T x <= b_i \tag{1}$$

where i is the index number of the convex hull. Furthermore, we can formulate the polyhedra $Poly$ as:

$$Poly := l_1 \cap l_2 ... \cap l_k \tag{2}$$

Since the $Poly$ is the common area of all the sample center positions of the latching mechanism on the USV. Therefore, there is a high chance that the power-supply socket will latch the mechanism within the common polyhedra area. We aim to improve the latching success rate by further finding the optimal position within the common area. The optimal center is also the chebyshev center defined as the center of the inscribed maximum ellipsoid within the $Poly$. The maximum ellipsoid covers the most of the polyhedra area and the optimal center is the farthest position from all the "dangerous" edges. Therefore, the optimal center is the solution considering all the sample positions as well as the highest chance to latch successfully for the power-supply socket. We define the ellipsoid E as:

$$E := Bu + d||u||_2 <= 1 \tag{3}$$

where B is the transformation matrix of the ellipsoid controlling the orientation and length of the ellipsoid and d is the offset vector from the origin. To get the optimal position, we formulate the problem to maximize the ellipsoid with respect to the position variable B and d as follows:

$$\begin{aligned} f(B,u) &= \max_{B,d} \ logdet(B) \\ s.t. \ ||Ba_i||_2 &+ a_i^T d <= b_i \\ D_{soc} &<= 2 * r_{obj} \end{aligned} \tag{4}$$

The first set of constraints are the boundaries of the polyhedra where all the solutions must be within it. The second set of constraints guarantee the optimal solution must be feasible to hold the power-supply pocket with diameter D_{soc}. Therefore, the power socket can always and successfully latch with the latching mechanism theoretically. The pipeline of the proposed vision-guided algorithm is shown in Algorithm 1.

To further explain the algorithm step 4, we use a unit circle u, and then apply an affine transformation Bu to get an ellipsoid E and then translate the ellipsoid $Bu + d$ it to the proper position to fit the polyhedra. Since the ellipsoid

Algorithm 1 Vision-Guided Algorithm for Latching.

Input:

The set of samples for center, C_s;
The radius of latching mechanism, R;
The diameter of the plug, D;

Pipeline:

With Input data, calculate the desired optimal location, x_c;

1: Find the intersection area $Intersec$ of sample center positions C_s with radius R;
2: Use convex hull $Hull$ to approximate the intersection area of sample circles with center C_s and radius R;
3: Formulate the convex hull $Poly$ using linear inequalities $L = l_1 \cap l_2 \cap ... \cap l_k,\ where\ i = 1, 2, ..., m$;
4: Formulate the objective problem using ellipsoid $E = \{Bu+d||u|| <= 1\}$ to maximize the feasible area inside the polyhedra with constraints L
5: **return** x_c, the maximum ellipsoid center and its radius r_{obj} with distribution probability $P_C(x)$;

must be within the constraints 3 in our algorithm, to cover the intersection area as much as possible, we maximize the ellipsoid size by using the optimization method. We formulate and solve optimization problem in 4 using convex optimization referring to [13].

Furthermore, the circle radius R of the intersection area is also the radius of the latching mechanism. It is a hyperparameter which we can evaluate based on the water environment and the size of the USV. Typically, the larger the design radius of the latching mechanism, the higher chance to perform the latching operation. However, this will also lead to more cost to retrofit the USV. To increase the latching success rate, different working scenarios are considered: (1) In severe water condition, a larger latching design radius is preferred. (2) In mild-severe water condition, a safer and effective strategy is stressed and implemented. First, we define a threshold $TD = \frac{1}{2} * R$, half of the design radius. Then we define TD_{new} as the distance between the last optimal center and the new optimal center. The TD_{new} value also represents the water disturbance level. If the disturbance $TD_{new} \geq TD$, it means the boat movement is wild and the docking success rate will decrease. In this situation, we recommend the strategy to resample the USV position and the optimal position will be recalculated, until it satisfies the threshold. (3) If the power supply socket fails to enter the latching mechanism in severe water condition, the ultrasonic sensor mounted at the base of the mechanism will detect the unsuccessful operation and similar recovery operation in scenario 2 will be reoperated.

IV. Latching Mechanism Design and Optimization

As depicted in Section II, our proposed system is a two-stage system. In Stage I, the vision-guided algorithm finds the optimal position in the disturbed water environments. Even with the estimated the optimal position for the USV to latch in Stage I, in this stage, the uncertain disturbance is further taken into consideration to achieve successful latching. In stage II, our designed latching mechanism will self-align the power-supply socket and further provide a more reliable and efficient latching.

A. Mechanical Design

We have a prerequisite in this work, that is, we consider to use a circular power interface which includes the circular power-supply socket and the power plug, as described in Section II. The mechanical design is inspired by the particle robotics [16], which can change the opening radius through a motion of opening or closing with no change the center of the circles.This feature can be utilized to eliminate the misalignments caused by the disturbance on the water. As for our proposed latching mechanism, it mainly consists of a driving gear, a driven gear with slots, three evenly distributed claws modules (the number can be up to six in this design) and a base with slots. As shown in Fig.5, the driving gear is driven by a stepper motor with reducer. Each claw includes a pin and a sliding table, and they are respectively fitted with the driven gear and the sliding slots of the base. The slots in base are perpendicular to the radial direction. The claws are constrained by the driven gear and also the slots of the base. So when the driving gear rotates, the claws can only move along the tangential direction, which makes the claws shift their states from opening to closing or vice versa. The motion range is determined by the length of slots.

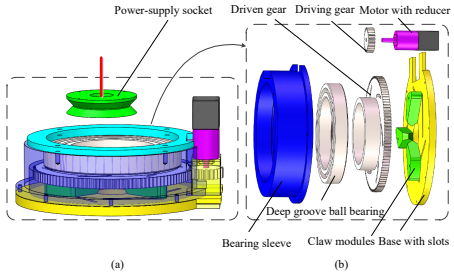

Fig. 5. The CAD design of automatic latching mechanism. (a) The power-supply socket and the assembly view of the latching mechanism. (b) The exploded view of the latching mechanism.

The design principle of this latching device is similar to the iris diaphragm structure in digital cameras, which is used to adjust the aperture size of the lens. Different from the iris diaphragm structure which is fully closed in the closing state, this latching mechanism reserves a circle space in the closing state. And this space is reserved for a circular power-supply socket. At first the radius of this circle space is greater than the power-supply socket. But once a power-supply socket enters into the space, the latching mechanism will perform the self-aligning operation to force the power-supply socket to the reserved circle space in the center. Furthermore, the slef-locking operation could shrink the radius and the latching mechanism will get to a locking state with the power-supply socket.

B. Self-aligning and Self-locking

Self-aligning can compensate for the misalignments caused by the disturbance that may still exist even after

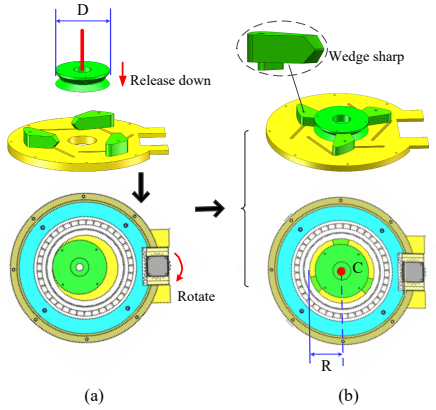

Fig. 6. The procedures of self-aligning and self-locking. (a) The claw modules are in an opening state. The power-supply socket goes down to the base, ready for charging. But there exists some misalignments. (b) The step motor rotates followed by the claw modules change to a closing state.

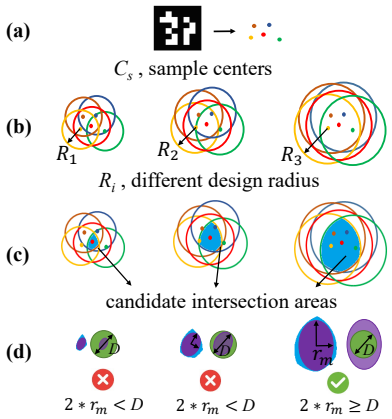

Fig. 7. Optimal radius design: (a) In a certain disturbance level, the proposed algorithm samples the centers C_s of the latching mechanism. (b) Different circles with design radius R_i are used to represent the latching mechanism movement area. (c) Overlapped circles lead to different candidate intersection areas. (d) The different candidate intersection areas are represented by ellipsoids. The intersection areas with R_i which can hold the power-supply socket D are the feasible design radius R_i.

Stage I. Therefore, it makes self-locking also an essential part of reliable latching operation. With self-aligning an self-locking operation, the power-supply socket will be locked in a particular predefined position and stay stable. Figure.6 illustrates how the mechanism finishes the procedures of self-aligning and self-locking of the power-supply socket within one step. Once the power-supply socket is released and goes down to the base, the stepper motor rotates and then the claw modules will shift to a closing state. Finally, the wedge-shaped ports of the three claws mesh with the power supply socket and remain in self-locking state. In the meantime, the misalignments are eliminated. Thus, this latching mechanism can further guarantee the reliable latching and there will be no relative motion between the power-supply socket and the USV.

C. Optimal Design Radius of The Latching Mechanism

In this section, we will discuss the design radius of the latching mechanism. As we have discussed in Section III, the latching design radius R is a hyperparameter we need to design. Our goal is to find an optimal design radius in guarantee of certain success rate. In this part, We will provide a methodology to find the maximal success rate as well as the minimal design radius based on the different disturbance levels. The methodology will provide guidance to design the radius of the latching mechanism.

As shown in Fig.7, similar to our vision-guided algorithm, different sizes of latching mechanism design radius R_i will form different candidate intersection areas based on the sample centers C_s from the outdoor experiments. The feasible intersection area should be large enough for the power-supply socket to go through. As shown in Fig.7, the rightmost intersection area with design radius R_3 is large enough to satisfy our needs. Therefore, if the design radius is larger than R_3, it is a feasible design radius. Furthermore, the algorithm implements the above principle to find the optimal radius R_{opt} in different disturbance levels $Dist$, given the diameter of the power-supply socket D and sample data C_s. Therefore, the R_{opt} can be expressed by the following function:

$$R_{opt} = \min f(C_s, D, Dist) \tag{5}$$

where f is a function that calculates a feasible radius. By minimizing the feasible radius, we can get the minimal radius R_{opt}.

In our experiments, the power-supply socket with diameter $D = 50mm$ will dock at the latching mechanism. In this case, we want to determine the optimal design radius in different disturbance levels. With the sample centers C_s of the USVs latching mechanism, different design radius R_i of latching mechanism are used to calculate the optimal design radius R_{opt} in different disturbance. The disturbance level $Dist$ is characterized by the IMU data which will be explained in Section V. This methodology will give us the optimal design radius in different disturbed environments. The design radius identification will be further explained in our experiments.

V. EXPERIMENTS AND EVALUATIONS

The main objectives in this section for our proposed latching system are: 1. validation of the feasibility of our proposed latching system. 2. improvement of the success rate using our system to perform latching operation and automatic charging for USVs. Therefore, our system is evaluated mainly in the following experiments: (1) The identification of optimized minimum radius R_{opt} in different disturbance levels on water. (2) The success rate of latching operation with and without the proposed algorithm in disturbances. The experiment setup is introduced first. Then the experiment of the latching mechanism radius design comes second and latching success rate results are shown finally.

A. Field Experiment Setup

The latching system consists of the following parts: the experiment platform is a USV 900mm in length and 600mm in width as shown in Fig. 1; An IMU (JY901) is used to collect pose and disturbance data on the USV; An ultrasonic

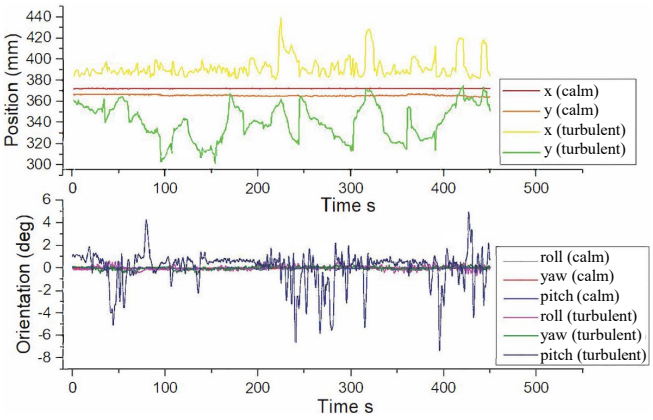

Fig. 8. IMU data in disturbance: position (x,y) and orientation (roll, yaw, pitch) data in calm and turbulent disturbances in a lake.

sensor continuously detects the height of the power-supply socket to judge whether the power-supply socket docks successfully.

All the experiments are conducted within the berth in the lake without considering the USV navigation and homing. The real-time experiment data of position and orientation is shown partly in Fig.8. Different disturbance levels are indicated by orientation and position data collected by the IMU sensors on the USV. By using just the same criteria as the outdoor latching experiments from a famous research project Roboat from MIT [11], we classify the disturbance environment into different levels as shown in Table.I and II by the offset in position and orientation. For now, our current research focuses on the latching systems within a berth in a lake, not in the open sea. But even in the current experiments, our experiments suffer from even wilder disturbance compared with the disturbance of that in [11] with the same sensor data criteria.

B. Identification of Minimum Design Radius of The Latching Mechanism

In this section, the identification of the optimal design radius procedure is done by calculating the success rate of different design radius R_i. Out of all the experiments in different disturbance levels, the success rate is defined as the percentage when the minor axis r_m of the ellipsoid area satisfies the condition $2 * r_m >= D$, namely larger than the power-supply socket size as shown in Fig.7. The optimal design radius is the radius when the success rate will not increase as the design radius R_i continues increasing. In the experiments, all the center data C_s and different radius R_i with their success rate are calculated by simulation using the outdoor disturbance data and the proposed optimal design radius methodology. The simulation result is shown in Table I.

From the results in Table I, the tendency shows the success rate continues to improve until a certain design radius. This certain design radius is the optimal radius R_{opt} we want. For example, in L3, the shift error is $(dx, dy) = (93.81, 88.13)$ and the success rate keeps improving as the design radius R_i increases from 60mm to 90mm. But after 90mm, the success rate will stay the same. This means the optimal design radius of the latching mechanism will be 90mm with 100% success rate. If you choose a larger design radius, there is no good to improve the success rate. This table provides a reference for designers to find the optimal radius in different disturbance levels.

To validate our methodology of optimal design radius for the latching mechanism, we design two different radius $R_1 = 75mm$ and $R_2 = 90mm$ and conduct the experiments in L3 with $R_1 = 75mm$ and L4 with $R_1 = 90mm$. The disturbance in L3 is milder than that in L4 as shown in Table I. The success rate theoretically in Table I should be 93.75% and 87.88% respectively. Taking L3 for example, the radius ranges from $75mm$ to $90mm$, the success rate increases synchronously. Considering the success rate, the first design radius $R_1 = 75mm$ provides a better design radius in L3 with higher success rate than $R_2 = 90mm$ in L4 even though R_1 is smaller than R_2. To achieve 100% success rate in L3, we should design radius larger than 90mm. Therefore, the algorithm can increase the efficiency of design the latching mechanism radius.

C. Latching Success Rate

With our proposed vision-guided positioning algorithm and self-aligning mechanism design, we conduct experiments to validate our automatic latching mechanism system for charging within the berth. The disturbance levels are classified using the IMU data sensor as explained in the outdoor experiment setup session. The (r, p, y) stands for the USV roll, pitch and yaw respectively. The (dx, dy) stands for the latching mechanism movement range of in position x and y as shown in Fig.4.

The results are shown in Table II with design radius $R_i = 90mm$ and power-supply socket diameter $50mm$. In all the 4 sets of 340 experiments in different disturbance levels, our system surpasses all the docking success rate without our system. Based on the historic sample center positions as illustrated in our algorithm 1 and Fig. 4, our algorithm is able to compensate the disturbance under disturbances. Together with the self-aligned latching mechanism, significant improvement of latching success rate has been obtained. In the best case, L4, the latching procedure success rate improves from 40% to 73.3%, as shown in Table II. Furthermore, by using our algorithm an optimal design radius will improve the efficiency of designing the latching mechanism radius by providing the guideline in Table I. The experiments validate our algorithm and system and the experiments significantly increase the latching success rate in disturbances.

VI. CONCLUSIONS AND FUTURE WORK

In this paper, to tackle with the challenging disturbance environments for the USV charging in berth, a vision-guided algorithm is proposed based on an intersection area of the historic positions. The vision-guidance algorithm gives the optimal position which works significantly in disturbed environment. Besides, the novel latching mechanism further compensates the misalignments caused by disturbances. In

TABLE I

OPTIMAL DESIGN RADIUS FOR THE LATCHING MECHANISM WITH THEIR SUCCESS RATE

	Design Radius R_i (mm)									
Disturbance Level (mm)		60	65	70	75	80	85	90	95	100
	L1 dx=1.18 dy=5.39	50/50 (100%)	50/50 (100%)	50/50 (100%)	50/50 (100%)	50/50 (100%)	50/50 (100%)	50/50 (100%)	50/50 (100%)	50/50 (100%)
	L2 dx=25.24 dy=83.96	41/50 (82%)	47/50 (94%)	49/50 (98%)	50/50 (100%)	50/50 (100%)	50/50 (100%)	50/50 (100%)	50/50 (100%)	50/50 (100%)
	L3 dx=93.81 dy=88.13	11/32 (34.38%)	25/32 (78.13%)	27/32 (84.38%)	30/32 (93.75%)	31/32 (96.88%)	31/32 (96.88%)	32/32 (100%)	32/32 (100%)	32/32 (100%)
	L4 dx=87.28 dy=134.95	7/33 (21.21%)	14/33 (42.42%)	17/33 (51.52%)	21/33 (63.64%)	23/33 (69.7%)	26/33 (78.79%)	29/33 (87.88%)	33/33 (100%)	33/33 (100%)

TABLE II

LATCHING EXPERIMENTS SUCCESS RATE

Level	Position (*mm*) and Orientation (*deg*) error	Success Rate without algorithm	Success Rate with algorithm
L1 Static	*(dx, dy)≈(1.18, 5.39)* *(r, p, y)≈(0.05, 0.09, 0.31)*	50/50 (100%)	50/50 (100%)
L2 Slight	*(dx, dy)≈(25.24, 83.95)* *(r, p, y)≈(0.54, 0.42, 7.36)*	40/50 (80%)	44/50 (88%)
L3 Moderate	*(dx, dy)≈(93.81, 88.13)* *(r, p, y)≈(1.15, 0.74, 3.61)*	44/50 (88%)	27/30 (90%)
L4 Wild	*(dx, dy)≈(87.28, 134.95)* *(r, p, y)≈(3.02, 2.07, 12.59)*	12/30 (40%)	22/30 (73.3%)

addition, our algorithm also presents a method to determine the optimal design radius of the latching mechanism. The proposed system has been validated with experiments in different disturbance levels and significantly improves the success rate.

In our future work, the proposed system will be further explored in larger USVs and the optimal radius design for latching mechanism can be further validated in more experiments. Also, we will pay attention on the problem of maintaining a reliable charging operation since the disturbance in the berth requires a sturdy connection. Our vision is to achieve full autonomy of latching and charging for the USVs community. By combining with the optimized size of latching mechanism, this solution has great potential for practical applications to enhance and boost the intelligence and autonomy of both the USVs and the smart ports.

REFERENCES

[1] Liu Z, Zhang Y, Yu X, et al. Unmanned surface vehicles: An overview of developments and challenges[J]. Annual Reviews in Control, 2016, 41: 71-93.

[2] Z. Kitowski and R. Soliński, "Application of domestic unmanned surface vessels in the area of internal security and maritime economy—capacities and directions for development," Scientific Journal of Polish Naval Academy, vol. 206, no. 3, pp. 67-83, 2016.

[3] Phamduy P, Cheong J, Porfiri M. An autonomous charging system for a robotic fish[J]. IEEE/ASME Transactions on Mechatronics, 2016, 21(6): 2953-2963.

[4] Devaraju A, Chen L, Negenborn R R. Autonomous Surface Vessels in Ports: Applications, Technologies and Port Infrastructures[C]//International Conference on Computational Logistics. Springer, Cham, 2018: 86-105.

[5] Wilson D B, Goktogan A H, Sukkarieh S. Experimental validation of a drogue estimation algorithm for autonomous aerial refueling[C]//2015 IEEE International Conference on Robotics and Automation (ICRA). IEEE, 2015: 5318-5323.

[6] Song G, Wang H, Zhang J, et al. Automatic latching system for recharging home surveillance robots[J]. IEEE Transactions on Consumer Electronics, 2011, 57(2): 428-435.

[7] Sato Y, Maki T, Masuda K, et al. Autonomous latching of hovering type AUV to seafloor charging station based on acoustic and visual sensing[C]//2017 IEEE Underwater Technology (UT). IEEE, 2017: 1-6.

[8] Martins A, Almeida J M, Ferreira H, et al. Autonomous surface vehicle latching manoeuvre with visual information[C]//Proceedings 2007 IEEE International Conference on Robotics and Automation. IEEE, 2007: 4994-4999.

[9] Dunbabin M, Lang B, Wood B. Vision-based latching using an autonomous surface vehicle[C]//2008 IEEE International Conference on Robotics and Automation. IEEE, 2008: 26-32.

[10] Scott G P, Henshaw C G, Walker I D, et al. Autonomous robotic refueling of an unmanned surface vehicle in varying sea states[C]//2015 IEEE/RSJ International Conference on Intelligent Robots and Systems (IROS). IEEE, 2015: 1664-1671.

[11] Mateos L A, Wang W, Gheneti B, et al. Autonomous latching system for robotic boats[C]//2019 International Conference on Robotics and Automation (ICRA). IEEE, 2019: 7933-7939.

[12] Wang J, Olson E. AprilTag 2: Efficient and robust fiducial detection[C]//2016 IEEE/RSJ International Conference on Intelligent Robots and Systems (IROS). IEEE, 2016: 4193-4198.

[13] Agrawal A, Verschueren R, Diamond S, et al. A rewriting system for convex optimization problems[J]. Journal of Control and Decision, 2018, 5(1): 42-60.

[14] Lin R, Li D, Zhang T, et al. A non-contact latching system for charging and recovering autonomous underwater vehicle[J]. Journal of Marine Science and Technology, 2019, 24(3): 902-916.

[15] Myint M, Yonemori K, Yanou A, et al. Dual-eyes visual-based sea latching for sea bottom battery recharging[C]//OCEANS 2016 MTS/IEEE Monterey. IEEE, 2016: 1-7.

[16] Li S, Batra R, Brown D, et al. Particle robotics based on statistical mechanics of loosely coupled components[J]. Nature, 2019, 567(7748): 361.

[17] Park D, Jung J, Kwak K, et al. 3D underwater localization using EM waves attenuation for UUV latching[C]//2017 IEEE Underwater Technology (UT). IEEE, 2017: 1-4.

[18] Myint M, Yonemori K, Yanou A, et al. Visual-servo-based autonomous latching system for underwater vehicle using dual-eyes camera 3D-pose tracking[C]//2015 IEEE/SICE International Symposium on System Integration (SII). IEEE, 2015: 989-994.

[19] Lwin K N, Mukada N, Myint M, et al. Visual latching Against Bubble Noise With 3-D Perception Using Dual-Eye Cameras[J]. IEEE Journal of Oceanic Engineering, 2018.

[20] Booij N, Ris R C, Holthuijsen L H. A third-generation wave model for coastal regions: 1. Model description and validation[J]. Journal of geophysical research: Oceans, 1999, 104(C4): 7649-7666.